Developmental Biology 406 (2015) 1–13

Contents lists available at ScienceDirect

Developmental Biology

journal homepage: www.elsevier.com/locate/developmentalbiology

Fertilization stimulates 8-hydroxy-2′-deoxyguanosine repair and antioxidant activity to prevent mutagenesis in the embryo

Tessa Lord *, R. John Aitken

Priority Research Centre for Reproductive Biology, School of Environmental and Life Sciences, University of Newcastle, Callaghan, NSW 2308, Australia

ARTICLE INFO

Article history:
Received 27 March 2015
Received in revised form
26 July 2015
Accepted 29 July 2015
Available online 30 July 2015

Keywords:
8-Hydroxy-2'-deoxyguanosine
Oxidative DNA damage
Zygote
Oocyte
Base excision repair

ABSTRACT

Oxidative DNA damage harbored by both spermatozoa and oocytes at the time of fertilization must be repaired prior to S-phase of the first mitotic division to reduce the risk of transversion mutations occurring in the zygote and subverting the normal patterns of cell differentiation and development. Of the characterised oxidative DNA lesions, 8-hydroxy-2′-deoxyguanosine (8OHdG) is particularly mutagenic. The current study reveals for the first time a marked acceleration of 8OHdG repair in the mouse oocyte/zygote by the base excision repair (BER) pathway following fertilization. Specifically, fertilization initiates post-translational modification to BER enzymes such as OGG1 and XRCC1, causing nuclear localisation and accelerated 8OHdG excision. Additionally, both the nuclear and mitochondrial genomes appear to benefit from increased protection against further 8OHdG formation by a fertilization-associated increase in glutathione peroxidase activity. The major limitation of the characterised 8OHdG repair system is the relatively low level of OGG1 expression in the oocyte, in contrast to the male germ line where it is the only constituent of the BER pathway. The male and female germ lines therefore collaborate in the repair of oxidative DNA damage, and oocytes are vulnerable to high levels of 8OHdG being carried into the zygote by the fertilizing spermatozoon.

1. Introduction

Repair of oxidative DNA damage within the one-cell zygote, prior to the initiation of S-phase of mitosis, is a critical step in the creation of viable embryos and healthy offspring. In the absence of successful repair of oxidative lesions such as 8-hydroxy-2'-deoxyguanosine (8OHdG), G-C to T-A transversion mutations (Wood et al., 1992) can occur during DNA replication that not only alter the genetic profile of the zygote itself but also every cell generated by the rapid mitotic divisions that characterize embryogenesis. Thus, transversion mutations within the zygote have the propensity to irreversibly alter gene expression profiles and thence the fidelity of normal embryonic development (Bruner et al., 2000; Wu et al., 2013; Ohno et al., 2014). Despite the importance of repairing oxidative DNA damage at this early stage of development, gametes harboring high levels of 8OHdG at the time of fertilization are known to undergo inadequate DNA repair in the zygote, resulting in detrimental effects on the pre-implantation development of the embryo (Takahashi, 2012; Lane et al., 2014) and on fetal growth and development (Chabory et al., 2009; Lane et al., 2014), as well as defects in offspring, including cancer and a significant reduction in lifespan (Ronen and Glickman, 2001; Vinson and Hales, 2002; Aitken et al., 2009).

Unfortunately, both spermatozoa and oocytes are known to harbor oxidative DNA lesions that can be contributed to the zygote following fertilization. The spermatozoon is particularly vulnerable to oxidative attack as a consequence of its propensity to produce reactive oxygen species (ROS) during the promotion of sperm capacitation (Aitken et al., 1995; Rivlin et al., 2004; O'Flaherty et al., 2006), its lack of antioxidant protection as a result of the restricted distribution and minimal volume of sperm cytoplasm, and a paucity of DNA repair mechanisms within a cell that possesses very little capacity for transcription or translation [reviewed by Aitken and De Iuliis (2010)]. Further to this, the increased utilization of assisted reproductive technologies (ART) such as ICSI to treat sub-fertile patient populations that are known to possess significantly elevated levels of 8OHdG in their spermatozoa (De Iuliis et al., 2009; Aitken et al., 2010) increases the likelihood that a spermatozoon harboring mutagenic lesions will achieve fertilization by bypassing a number of natural selection strategies that would normally be operating in vivo.

As a consequence of the spermatozoon's purported deficiency in DNA repair capacity, the responsibility for resolving the oxidative lesions contributed to the zygote by both male and female gametes is traditionally thought to lie entirely with the oocyte (Shimura et al., 2002). Single nucleotide repair of 8OHdG lesions in

* Corresponding author. Fax: +61 2 4921 6308.
E-mail address: tessa.lord@uon.edu.au (T. Lord).

http://dx.doi.org/10.1016/j.ydbio.2015.07.024
0012-1606/

eukaryotic cells is primarily conducted by the base excision repair (BER) enzymes: oxoguanine glycosylase (OGG1), apurinic/apyrimidinic endonuclease (APE1) and X-ray repair cross complementing protein (XRCC1). Although repair of oxidatively damaged DNA can also be conducted by the enzymes of the nucleotide excision repair (NER) pathway, this complex, multistep repair process is generally reserved for lesions that are causing structural distortion of the DNA (Brierley and Martin, 2013). Within the BER pathway, recognition of the 8OHdG adduct and subsequent base excision is performed by the DNA glycosylase OGG1. The residual abasic site is then hydrolyzed by the endonuclease APE1, allowing for replacement of the purine or pyrimidine base by polymerase β. Ligation of the strand nick is then performed by DNA ligase in association with the scaffolding protein XRCC1 [reviewed by David et al. (2007)]. Indeed, the oocyte is known to accumulate an abundance of mRNA's and proteins involved in DNA repair within its vast cytoplasm during oogenesis (Zheng et al., 2005; Menezo et al., 2007), as the opportunity to transcribe new DNA repair genes is not available to the embryo until the 2-cell stage in the mouse (Flach et al., 1982), and the 4-cell stage in humans (Braude et al., 1988).

In reality however, repair of oxidative DNA damage potentially involves a measure of co-operation between male and female gametes prior to the initiation of embryo development. The first enzyme of the BER pathway, OGG1, has been clearly identified in the chromatin of human spermatozoa (Smith et al., 2013b). This sperm-derived OGG1 was not only found to be present at both the mRNA and protein level, but was also capable of cleaving 8OHdG adducts from sperm nuclear DNA to create the corresponding abasic sites. Despite the presence of OGG1 in sperm chromatin, the subsequent enzymes of the BER pathway, APE1 and XRCC1, could not be identified within human spermatozoa suggesting that this repair pathway can only be driven to completion by the oocyte, post-fertilization (Smith et al., 2013b).

The current study utilizes a mouse model to characterize BER in the zygote, prior to the initiation of S-phase, with a particular focus on the potential for collaboration between sperm- and oocyte-derived BER enzymes. The results reveal a previously unappreciated upregulation of 8OHdG repair following fertilization as result of maternally driven post-translational modification to selected BER enzymes. Additionally, a fertilization-associated increase in antioxidant activity that decreases vulnerability of the zygote to oxidant-induced DNA damage was characterized. Cumulatively, these molecular mechanisms are likely to be critically important for protecting the genetic integrity of the zygote to allow for unimpeded transition through embryogenesis. However, low levels of OGG1 expression detected within the murine oocyte in this study highlight the vulnerability of the zygote to mitotic progression in the absence of absolute DNA repair, as well as the necessity of OGG1 activity in the sperm cell prior to fertilization to lower the burden of 8OHdG repair on the oocyte.

2. Materials and methods

2.1. Chemicals and materials

All chemicals were purchased from Sigma-Aldrich (St Louis, MO, USA) unless otherwise stated. Anti-XRCC1 antibody was purchased from Epitomics (Littleton, CO, USA) (catalog number 3631-1), while antibodies against OGG1, APE1, phosphorylated XRCC1 (phospho S518, T519 and T523) and PMP70 were purchased from Abcam (Cambridge, UK) (ab91421, ab194, ab84417 and ab3421 respectively). Anti-phospho-serine (P5747) and - phosphothreonine (P6623) antibodies were both from Sigma-Aldrich.

2.2. Oocyte collection

Three to four week old C57BL6/CBA F1 female mice were subjected to a superovulation regime and oocytes were collected and denuded as described previously (Lord et al., 2013). The use of animals in this project was approved by the University of Newcastle Animal Care and Ethics Committee, and all animals were obtained from breeding programs run in the University of Newcastle Central Animal House.

2.3. In vitro fertilization (IVF)

IVF was performed as described previously (Lord et al., 2013) using spermatozoa from 8 week old Swiss mice, or from the OGG1-deficient senescence-accelerated mouse prone 8 (SAMP8) (Choi et al., 1999) or senescence-resistant control strain of mouse, SAMR1. At 4 h post-insemination successful fertilization was determined via identification of the second polar body and/or formation of pronuclei.

2.4. Reverse transcription PCR (RT-PCR) and quantitative PCR (qPCR) of OGG1, APE1 and XRCC1

RNA extraction and reverse transcription were conducted as described previously (Sobinoff et al., 2013). Briefly, 2 μg of total RNA was extracted from a pooled population of oocytes, DNase treated to remove genomic DNA, and reverse transcribed with oligo(dT) primer (Promega, Madison, WI, USA) and M-MLV Reverse Transcriptase (Promega). Reverse transcription was verified by RT-PCR using cDNA amplified with GoTaq Flexi (Promega). All primers utilized have been provided in a supplementary data table (Supplementary Table S1). These primers were screened for specificity via a nucleotide BLAST search (NCBI) prior to use. Quantitative PCR was conducted using SYBR Green GoTaq qPCR master mix (Promega) over 40 amplification cycles on a LightCycler 96 SW 1.0 (Roche Diagnostics, Mannheim, Germany). LightCycler Analysis Software (Roche) was used to quantify SYBR Green fluorescence after each amplification cycle. The optimal annealing temperature for OGG1, APE1 and XRCC1 was 57 °C, as determined via a calibration curve, with all primer efficiencies lying between 1.8 and 2. Quantification of transcript abundance within oocytes was calculated relative to two housekeeping control genes, beta-2 microglobin (B2M) and beta-glucuronidase (Gusβ), which display similar primer efficiencies at 57 °C. A negative control in which reverse transcriptase had been omitted was also performed for each qPCR replicate.

2.5. Immunocytochemistry

Oocytes/zygotes were washed 4 × in PBS containing 3 mg/ml polyvinylpyrrolidone (PVP) prior to fixation in 3.7% paraformaldehyde for 1 h at room temperature (RT). Following fixation, oocytes were again washed in PBS/PVP before permeabilization in 0.25% Triton-X for 10 min at RT. Oocytes were then washed in PBS/PVP and blocked in 3% BSA/PBS for 1 h at 37 °C. Following this blocking step, oocytes were incubated in the desired primary antibody (all used at a concentration of 1/100 in 1% BSA/PBS) overnight at 4 °C before washing with 1% BSA/PBS and incubating in anti-rabbit Alexa Fluor 488 (1/1000) for 1 h at 37 °C. Immunofluorescence was observed using confocal microscopy (Olympus FV1000 confocal microscope; Notting Hill, VIC, Australia). Quantification of levels of fluorescence within oocytes was achieved using the public sector program ImageJ (US National Institutes of Health).

Immunocytochemistry was carried out on spermatozoa as described by Smith et al. (2013b), using hydrogen peroxide (H_2O_2)

and dithiothreitol to de-condense the highly compacted chromatin, and using primary antibodies within the same conditions described for oocytes.

2.6. SDS-PAGE and western blotting

Protein extraction was achieved by adding sodium dodecyl sulfate (SDS) extraction buffer (2% w/v SDS, 10% w/v sucrose in 0.1875 M Tris, pH 6.8) to cells and incubating at 100 °C for 5 min. The samples were then centrifuged (500*g* for 5 min) and the supernatant stored at −20 °C prior to use. Extracted proteins were loaded onto an SDS polyacrylamide gel (10 μg sperm protein per lane, or protein lysate from 100 oocytes per lane) and separated via electrophoresis. 1 μg of recombinant OGG1 (rOGG1), recombinant APE1 (rAPE1) (both from New England Biolabs, Ipswich, MA, USA), and Jurkat whole cell lysate (Novus Biologicals, Littleton, CO, USA) was loaded onto the polyacrylamide gels as a positive control for OGG1, APE1 and XRCC1 antibodies respectively. Following electrophoresis, proteins were transferred to a nitrocellulose membrane using standard Western transfer techniques. The nitrocellulose membrane was blocked with 5% skim milk for 1 h and washed 3 × in TBS containing 0.1% Tween (TBST). Blots were then incubated overnight at 4 °C with the appropriate primary antibody diluted in 1% skim milk in TBST. Primary antibodies were used at the following concentrations; OGG1-1/500, APE1-1/2000, XRCC1-1/5000. Blots were washed free from primary antibody in TBST, and incubated in goat anti-rabbit IgG-HRP (Sigma-Aldrich) secondary antibody (1/1000 in 1% skim milk/TBST) for 1 h at RT. Membranes were developed using an enhanced chemiluminescence kit (GE Healthcare, Castle Hill, Australia) according to the manufacturer's instructions.

2.7. Detection of extracellular 8OHdG – ELISA assay

A DNA oxidative damage ELISA kit (Cayman chemical, Ann Arbor, MI, USA) that is capable of detecting 8OHdG released into the extracellular space following excision by the cell's DNA repair machinery was utilized to assess levels of 8OHdG repair in the oocyte pre- and post-fertilization. Following the retrieval and denuding of oocytes, half were subjected to IVF, while half of the oocytes remained unfertilized. Following a 4 h incubation, oocytes were treated with 1 mM H_2O_2 for 1 h to induce 8OHdG formation. Upon removal of oocytes/zygotes from their respective media and assessment of fertilization rate, the culture media was collected and stored at −80 °C until required. The ELISA assay was carried out as per the manufacturer's instructions, and absorbance was read using a Fluostar Optima spectrophotometer (BMG Lab-Technologies, Durham, NC, USA). Values of 8OHdG release into the extracellular space are reported as pg/ml, normalized to the number of oocytes in each droplet. Fertilization rate was factored into calculations when formulating a per-oocyte value in 'fertilized' treatments, and replicates were only included where fertilization rate was over 80%.

2.8. Detection of intracellular 8OHdG in the oocyte and zygote and vitality assessment

In order to assess levels of intracellular 8OHdG in oocytes and zygotes, an OxyDNA test was conducted (Argutus Medical, Dublin, Ireland). Following the 4 h incubation to allow for fertilization and the 1 h incubation in 1 mM H_2O_2, cells were either subjected to fixation for the OxyDNA test or cultured for an additional 3 h 'recovery' period in M2 medium before being assessed for vitality using 50 μg/ml propidium iodide.

Fixation for the OxyDNA test was carried out in 3.7% paraformaldehyde overnight at 4 °C. The following day, oocytes and zygotes were permeabilized in 0.25% Triton-X in PBS for 10 min at RT. Oocytes/zygotes were then incubated for 1 h at 37 °C in OxyDNA reagent (1:100 dilution; as per the manufacturer's instructions). Finally, cells were counterstained for 5 min with propidium iodide before mounting for analysis by fluorescence microscopy. Pixel intensity values reflecting 8OHdG levels in oocytes and zygotes were generated using ImageJ in order to create a comparison between treatments.

2.9. Pharmacological inhibitor studies

Inhibitors of both the BER pathway ["BER inhibitor" (Merck, Darmstadt, Germany)], and NER pathway [X80 (Sigma-Aldrich)] were utilized at doses which have been previously recognized to be effective. Oocytes were exposed to either 10 μM of the BER inhibitor (Madhusudan et al., 2005), 100 μM X80 (Neher et al., 2010), or the equivalent concentration of DMSO, throughout the 4 h incubation which allowed for fertilization, as well as throughout the 1 h H_2O_2 treatment. Following this culture time, culture media was collected for analysis via the 8OHdG ELISA assay and zygotes were fixed and subjected to the OxyDNA test, followed by pixel intensity analysis using ImageJ.

Inhibition of CK2 in order to impair phosphorylation of XRCC1 (Parsons et al., 2010) was also conducted as described above. Oocytes were exposed to 4,5,6,7-Tetrabromo-2-azabenzimidazole (TBB) throughout the culture period initially in a dose – dependent manner (0–1000 μM) and finally at an effective but non-lethal concentration of 100 μM. Following incubation, culture media were again collected for ELISA analysis and oocytes were subjected to immunocytochemistry (see above) using the phospho-XRCC1 antibody.

Finally, 20 μg/ml cycloheximide was used as an inhibitor of translation/protein synthesis (Schneider-Poetsch et al., 2010) in the manner described above in order to further elucidate the mechanisms of increased 8OHdG excision post-fertilization.

2.10. Duolink – proximity ligation assay (PLA)

A Duolink in situ fluorescence PLA (Sigma-Aldrich) was used to identify phosphorylation of the BER enzymes at specific residues in the absence of commercially available phospho-antibodies. Oocytes and zygotes were fixed and permeabilized as detailed above (see *Immunocytochemistry*) before conducting the Duolink PLA preparation, detection, and analysis procedures as per the manufacturer's instructions. In the circumstance that two antibodies, such as those against OGG1 and phosphoserine, localize to the same target within the oocyte (< 30 nm distance), a punctate region of red fluorescence is emitted. In order to confirm that fluorescence detected within these experiments was not a result of non-specific binding or background signals, a series of technical and biological controls were carried out. These included the omission of one antibody, and conducting the assay between our antibodies of interest and an unrelated antibody with which they are not expected to interact, in this case, α-tubulin.

2.11. Assessing levels of ROS/antioxidant activity within the MII stage oocyte and zygote

In order to assess levels of ROS, and to make inference as to the antioxidant capacities of oocytes and zygotes following H_2O_2 treatment, a 5'-carboxy-2',7'-difluorodihydrofluorescein diacetate (DFF DA probe) (Molecular Probes, Eugene, OR, USA) was utilized. Untreated and 1 mM H_2O_2 treated MII stage oocytes and zygotes were incubated in a 10 μM solution of DFF DA in M2 media for 30 min at 37 °C. Oocytes were then washed 3 × before mounting for analysis by fluorescence microscopy using a Zeiss Axioplan

2 fluorescence microscope (Carl Zeiss MicroImaging Inc., Sydney, Australia). Quantification of average fluorescence levels between treatments was conducted using ImageJ pixel intensity analysis.

An antibody against the peroxisomal membrane marker PMP70 was used to identify any alterations to peroxisomal abundance – and thus catalase activity – within the oocyte pre- and post-fertilization (see *Immunocytochemistry*). Additionally, a glutathione peroxidase (GPx) assay kit (Cayman chemical) was used to assess GPx activity in populations of MII oocytes and zygotes (50 oocytes in each population). Lysates were prepared as per the manufacturer's instructions and absorbance was read using a Fluostar Optima spectrophotometer.

2.12. Statistical analyses

All experiments were conducted at least 3 × on independent samples and results were analysed by ANOVA using JMP version 9.0.0. A post hoc comparison of group means was conducted using a Fisher's Protected Least Significant Difference test. Analysis of paired samples was conducted using a paired Student's *t*-test. A value of $P < 0.05$ was considered to be statistically significant.

3. Results

3.1. OGG1 is under-represented in the murine oocyte, potentially affecting functionality of the BER pathway

In order to investigate the functionality of the BER enzymes in the mammalian oocyte and zygote, qualitative and quantitative analyses were conducted on the key enzymes within this pathway: OGG1, APE1 and XRCC1. As reported by microarray analyses conducted on MII stage oocytes from the rhesus monkey (Zheng et al., 2005), our study has demonstrated an under-representation at the transcript level of the first enzyme in the BER pathway (OGG1) within C57BL6/CBA mouse oocytes. Quantitative PCR

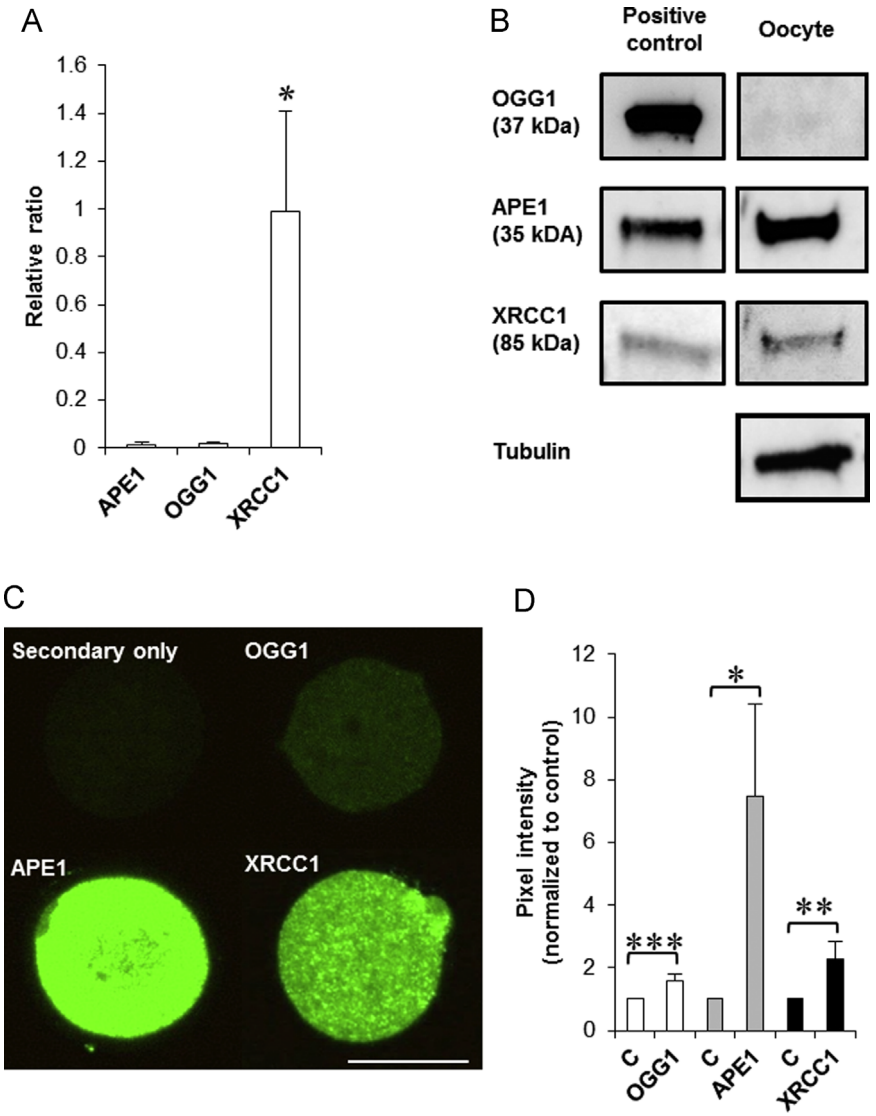

Fig. 1. OGG1 is under-represented in MII-stage mouse oocytes. (A) Quantitative PCR analysis revealed a low abundance of OGG1 and APE1 mRNA within the murine oocyte (relative to B2M and Gusβ), whilst XRCC1 transcripts were present at significantly higher levels. (B) Immunoblotting analysis of the protein composition of these oocytes identified bands corresponding to APE1 and XRCC1 at 35 kDa and 85 kDa respectively; whilst a 37 kDa band corresponding to OGG1 could not be detected at this concentration of protein (100 oocytes per lane, equivalent to ~1 μg protein). Positive controls; rOGG1, rAPE1 and Jurkat cell lysate respectively (~1 μg). (C, D) In support of Western blotting data, immunocytochemistry identified fluorescence associated with APE1 and XRCC1 throughout the ooplasm. Fluorescence relating to OGG1 was low, however upon pixel intensity analysis was still found to be significantly greater than the 'secondary only' control ("C"). Scale bar = 50 μm. Mean ± SEM values are plotted in histograms. Independent replicates were conducted with a minimum of 40 oocytes per replicate. $^{*}P < 0.05$, $^{**}P < 0.01$, $^{***}P < 0.001$.

analysis revealed low levels of both OGG1 and APE1 mRNA within MII stage oocytes, relative to the selected housekeeping genes B2M and Gus β, while XRCC1 was expressed at significantly higher levels ($P < 0.05$) (Fig. 1A). Importantly, analysis at the protein level revealed a similar trend in terms of OGG1 expression. Western blotting techniques demonstrated the presence of both APE1 and XRCC1 within oocyte lysates (100 oocytes per lane, approximately 1 μg protein) at 35 kDa and 85 kDa respectively; whilst no distinct band associated with OGG1 expression could be detected at 37 kDa at this protein concentration (Fig. 1B). Expression of each BER enzyme in oocyte lysates was compared to a positive control (1 μg): recombinant OGG1 (rOGG1), recombinant APE1 (rAPE1) or jurkat cell lysate for the XRCC1 antibody. In a similar fashion to our Western blotting analyses, immunocytochemistry revealed high levels of fluorescence associated with APE1 and XRCC1 dispersed throughout the ooplasm, while the fluorescence associated with OGG1 was low (Fig. 1C). Despite this, pixel intensity analysis revealed that levels of fluorescence associated with the OGG1 antibody were significantly elevated above that of the secondary only control ($P < 0.001$) (Fig. 1D), suggesting that this enzyme is still present within the oocyte, albeit at low levels. It should be noted that in addition to OGG1 being under-represented in comparison to APE1 and XRCC1 within the mammalian oocyte itself, a comparison of oocyte protein lysates to equivalent concentrations of protein from other tissue types (spleen and whole ovary protein lysates) revealed that OGG1 concentrations are up to 50% lower in oocyte lysates than that of the alternative tissue types observed (Supplementary Fig. 1).

Following this investigation of the BER enzymes, an analysis of the oocyte's capacity for 8OHdG repair was conducted. Despite the under-representation of OGG1 within MII stage oocytes, ELISA analysis did detect the release of 8OHdG into the extracellular space (oocyte culture media), suggesting that some capacity for OGG1-mediated 8OHdG excision does exist (Fig. 2A). Interestingly however, one-cell stage zygotes exhibited a superior capacity for 8OHdG excision compared with unfertilized MII stage oocytes; excising and releasing significantly higher levels of 8OHdG into the extracellular space ($P < 0.001$) following a 5 h incubation period that allowed for in vitro fertilization and included terminal exposure to 1 mM H_2O_2 for 1 h. (Fig. 2A). This highly significant increase in 8OHdG release was not an artifact created by the presence of spermatozoa within the 'fertilized' oocyte culture medium, as levels of 8OHdG release into the extracellular space within the 'sperm only' control were significantly lower than the increase observed between the MII and zygotic stages (Fig. 2A). To complement these ELISA data describing 8OHdG levels in the extracellular space, analysis of intracellular 8OHdG levels using an oxidative DNA damage assay revealed distinct variations between

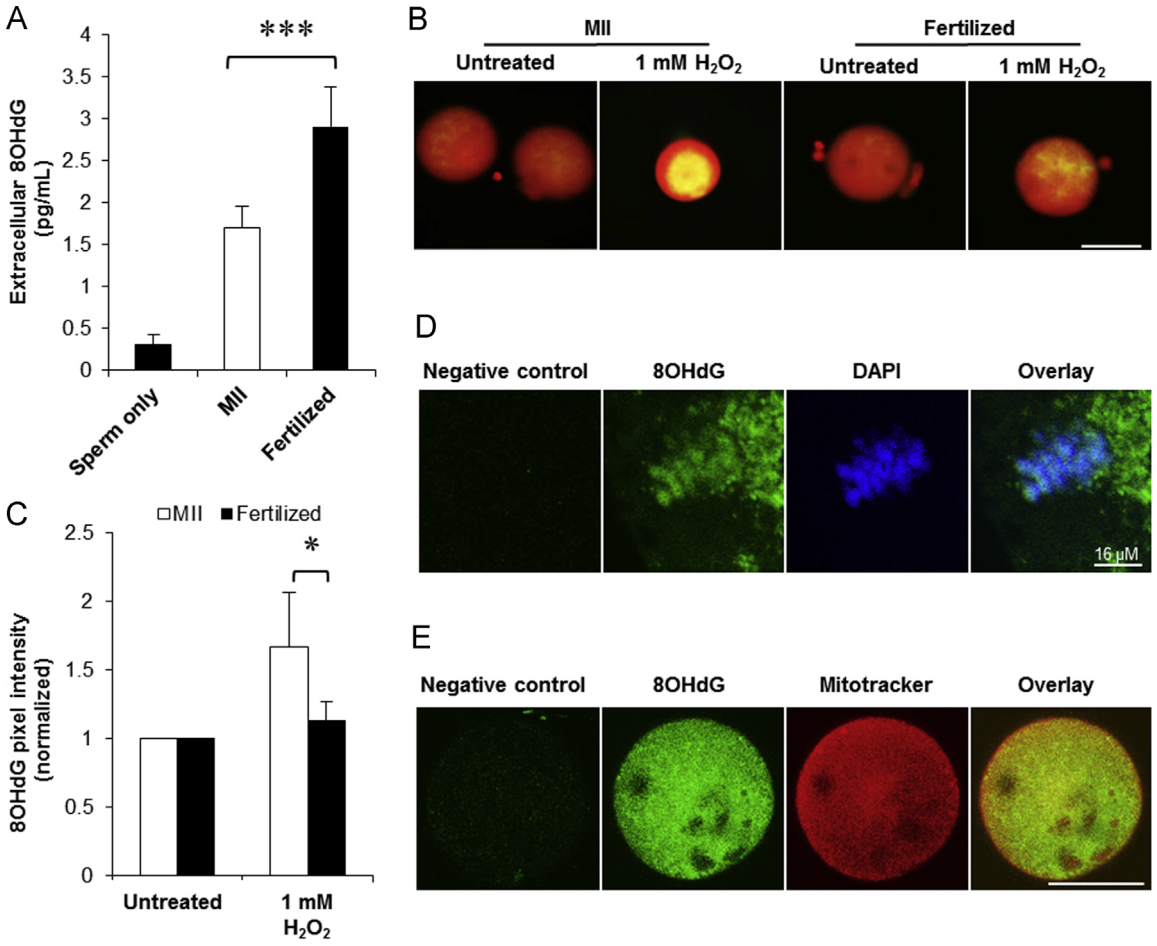

Fig. 2. Repair of oxidative DNA damage is accelerated within the oocyte post-fertilization. (A) Following insemination and a 1 h exposure to H_2O_2, fertilized oocytes exhibited significantly higher levels of 8OHdG excision and release into the extracellular space than unfertilized oocytes. (B, C) Additionally, MII oocytes experienced a prominent increase in levels of intracellular 8OHdG (indicated by FITC staining in representative images, red counterstain-propidium iodide) following H_2O_2 treatment, whilst fertilized oocytes exhibited little change in levels of oxidative DNA damage. Upon analysis of pixel intensity values, MII oocytes were found to contain significantly elevated levels of intracellular 8OHdG above fertilized oocytes following H_2O_2 treatment. (D) Representative image of 8OHdG fluorescence co-localizing with the metaphase plate (DAPI) following H_2O_2 treatment. (E) Fluorescence associated with 8OHdG was also found to co-localize with the mitochondrial DNA, as depicted by the Mitotracker red fluorescent probe. Scale bar = 50 μm. Mean ± SEM values are plotted in histograms. Independent replicates were conducted with a minimum of 40 oocytes per replicate. $^{*}P < 0.05$, $^{***}P < 0.001$.

pre- and post- fertilization oocytes. The OxyDNA assay revealed significantly lower levels of 8OHdG within H_2O_2 treated zygotes compared with MII stage oocytes ($P<0.05$) (Fig. 2B and C), with 8OHdG being identified within both the nuclear DNA (metaphase plate) (Fig. 2D) and the mitochondrial DNA (Fig. 2E); as demonstrated by co-localisation between the 8OHdG probe and the nuclear stain DAPI for the former, and Mitotracker red for the latter.

These data suggested that while repair of oxidative DNA damage is minimal in the MII oocyte due to low levels of OGG1, fertilization is associated with an accelerated rate of 8OHdG excision and extracellular release, suggesting upregulation of the BER pathway. Additionally, these data could also reflect a change in antioxidant activity within the oocyte post-fertilization.

3.2. Fertilization-associated increases in 8OHdG excision are orchestrated by the BER pathway, however unlikely to be reliant on sperm-derived OGG1

The investigation next focused on the characterization of mechanisms orchestrating the acceleration of 8OHdG repair in the zygote prior to the initiation of S-phase. Firstly, the observed elevation in 8OHdG excision was confirmed to be a result of BER enzyme activity. Impairment of the BER pathway was achieved via utilization of a commercially available pharmacological inhibitor ('BER inhibitor'). Exposure to the BER inhibitor (10 μM) throughout the 5 h incubation period prevented the fertilization-associated elevation in 8OHdG excision ($P<0.05$) (Fig. 3A). Additionally, the OxyDNA assay also revealed an elevation in levels of intracellular 8OHdG when oocytes were treated with the BER inhibitor in conjunction with H_2O_2 ($P<0.01$) (Fig. 3B). Contrastingly, oocytes which were exposed to an inhibitor of the NER pathway, X80 (Neher et al., 2010), continued to exhibit an acceleration of 8OHdG excision post-fertilization (Fig. 3C) and experienced no change from control oocytes in intracellular 8OHdG levels in response to H_2O_2 treatment (Fig. 3D). It should be noted that both the inhibitors utilized were observed to have no demonstrable effect on fertilization rate or viability of oocytes.

Given the apparent acceleration of BER observed in the early zygote, we next endeavored to determine whether this upregulation was a consequence of the OGG1 contributed to the zygote by the fertilizing spermatozoon. Firstly, immunocytochemistry/immunoblotting techniques were utilized to verify that, as in human

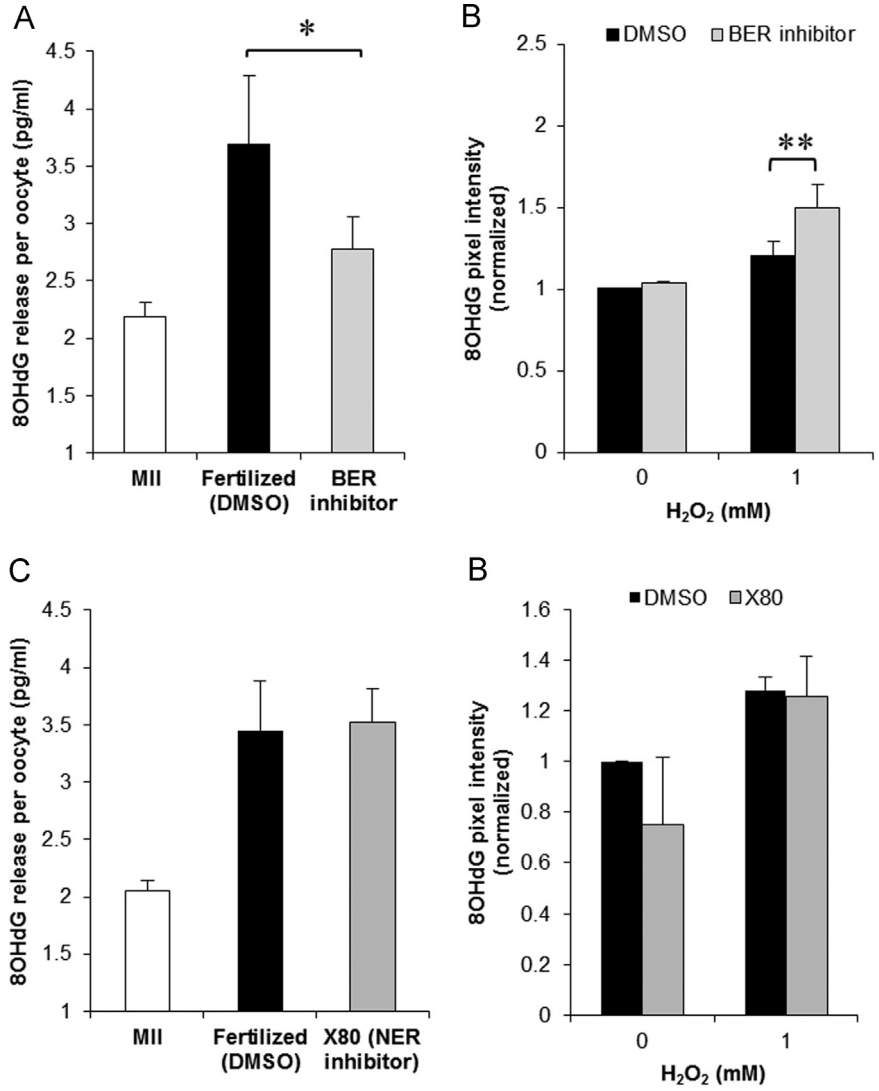

Fig. 3. The BER enzymes are responsible for the accelerated excision of 8OHdG post-fertilization. (A) Pharmacological inhibition of the BER pathway using a commercially available compound 'BER inhibitor' dampened the accelerated 8OHdG excision associated with fertilization, as determined by the ELISA assay. (B) Similarly, exposure to the BER inhibitor in conjunction with H_2O_2 resulted in a significant increase in levels of intracellular 8OHdG in zygotes. (C) In contrast, inhibition of the NER pathway using X80 did not affect the fertilization-associated up-regulation of 8OHdG excision, nor levels of intracellular 8OHdG (D). Intracellular 8OHdG values are normalized to the untreated control. Mean ± SEM values are plotted in histograms. Independent replicates were conducted with a minimum of 60 oocytes per replicate. $^{*}P<0.05$, $^{**}P<0.01$.

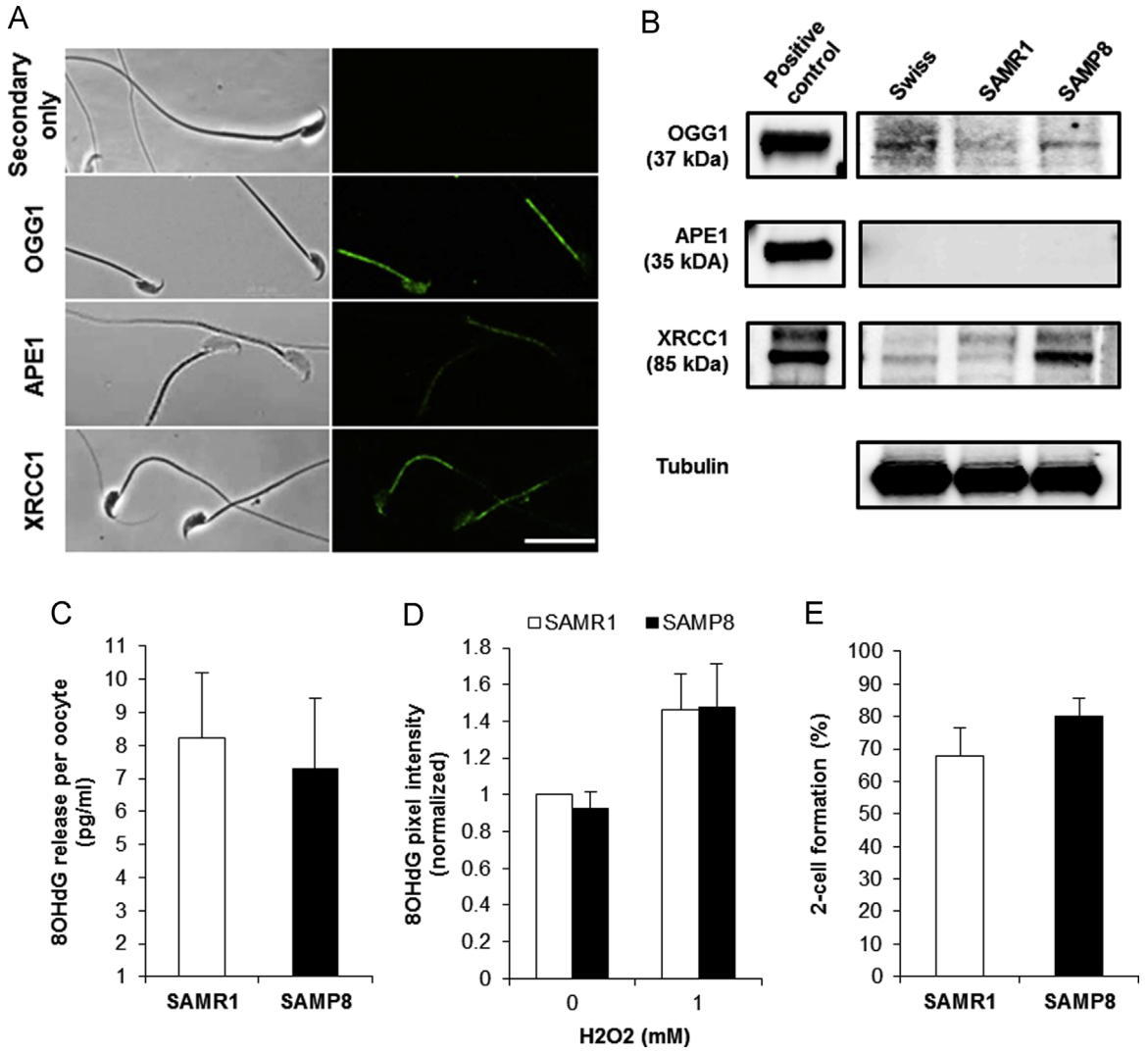

Fig. 4. OGG1 is present in mouse spermatozoa however is unlikely to be responsible for the acceleration of 8OHdG excision associated with fertilization. (A) Immunocytochemistry revealed OGG1 within the nucleus of the mouse spermatozoon, as previously reported in human sperm. APE1 could only be identified in the midpeice (mitochondria) of the sperm cell, whilst XRCC1 was identified within the midpiece, with some punctate staining within the nucleus. (B) Western blot analyses using sperm protein lysates (swiss, SAMR1 and SAMP8 mice) revealed that whilst OGG1 and XRCC1 are present, the pathway is truncated due to the absence of the endonuclease enzyme APE1. (C) Pronuclear stage zygotes produced via fertilization of wild type oocytes with sperm from either SAMR1 (control) mice, or OGG1-deficient SAMP8 mice, did not exhibit any changes in 8OHdG excision, suggesting that sperm-derived OGG1 is unlikely to orchestrate the burst of 8OHdG repair observed post-fertilization. (D) Similarly, zygotes derived from SAMP8 sperm did not exhibit elevated levels of intracellular 8OHdG above SAMR1-derived zygotes following H_2O_2 treatment. (E) Additionally, wild type oocytes fertilized with OGG1-deficient SAMP8 sperm did not display any impairment in developmental progression to the 2-cell stage. Scale bar=20 μM. Mean ± SEM values are plotted in histograms. Independent replicates were conducted with a minimum of 50 oocytes per replicate.

spermatozoa, murine spermatozoa possessed a truncated BER pathway characterized by the presence of the OGG1 enzyme but lacking APE1 and XRCC1. As predicted, immunocytochemistry identified the presence of OGG1 within both the nucleus (sperm head) and midpiece (mitochondria), whilst APE1 was identified only within the mitochondria, and XRCC1 primarily within the mitochondria with some punctate staining within sperm nuclei (Fig. 4A). Similarly, both OGG1 and XRCC1 were identified by Western blotting analysis in sperm protein lysates; however APE1 could not be detected (Fig. 4B) as a consequence of very low levels of expression, solely in association with the mitochondria.

In order to determine whether the OGG1 present in sperm chromatin is responsible for the increased 8OHdG excision observed, we utilized spermatozoa from the SAMP8 mouse which possesses severely defective OGG1 [10–40% of the activity exhibited by the senescence-resistant (SAMR1) control mouse] as a consequence of an arginine to tryptophan mutation at codon 304 (Choi et al., 1999). Importantly, this impairment in OGG1 enzyme activity has been confirmed to exist in the spermatozoa of SAMP8 mice (Smith et al., 2013a). Despite this, fertilization of wild type oocytes with these OGG1-deficient SAMP8 spermatozoa did not influence the accelerated 8OHdG excision associated with fertilization, as detected by the ELISA assay (Fig. 4C). Similarly, levels of intracellular 8OHdG were not observed to be significantly elevated in zygotes derived from SAMP8 sperm (Fig. 4D), and developmental progression to 2-cell stage was not hindered (Fig. 4E). Although it is possible that very low levels of functional OGG1 contributed to the oocyte by the fertilizing spermatozoon (such as those contributed by SAMP8 sperm) are sufficient to drive the observed rise in 8OHdG repair, with wild type sperm providing an 'excess' of protein that is not necessarily required, it is more plausible that maternally-derived factors are orchestrating this acceleration of BER in response to fertilization-associated cues.

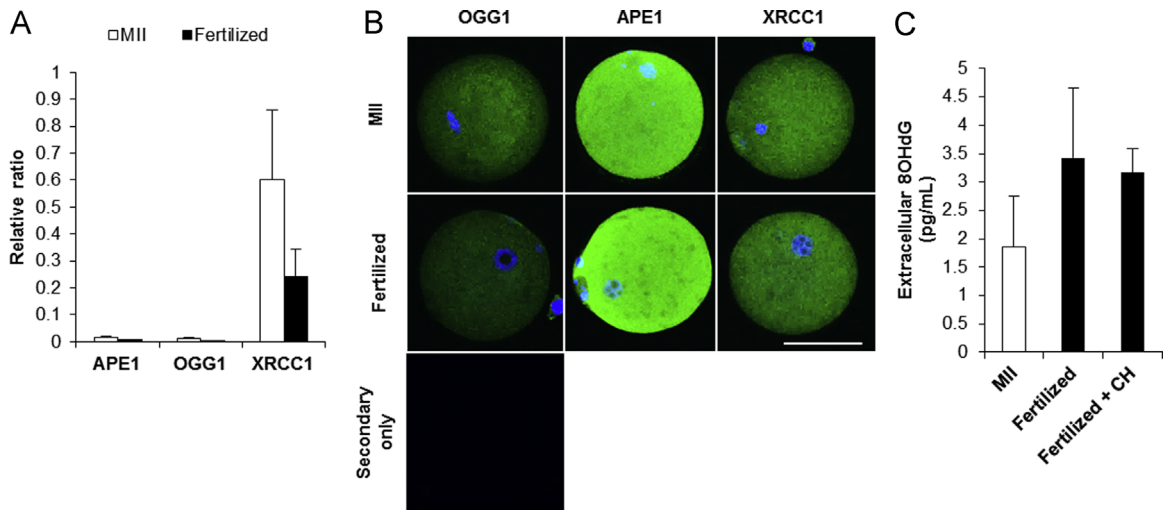

Fig. 5. Accelerated 8OHdG repair post-fertilization is not attributed to up-regulated expression of the BER enzymes. (A) Quantitative PCR analysis revealed no significant elevation in OGG1, APE1 or XRCC1 transcript levels (relative to B2M and Gusβ) following fertilization. (B) Similarly, no visible changes in fluorescence could be detected via immunocytochemistry when comparing OGG1, APE1 and XRCC1 in MII stage oocytes and zygotes. (C) Exposure to the translation/protein synthesis inhibitor cycloheximide (CH) throughout fertilization did not inhibit the fertilization-associated elevation in 8OHdG excision, thereby; increased expression of the BER enzymes could not be responsible for the acceleration of 8OHdG excision observed following fertilization. Mean ± SEM values are plotted in histograms. Independent replicates were conducted with a minimum of 60 oocytes per replicate. Blue staining = DAPI. Scale bar = 50 μm.

3.3. *Post-translational modifications instigate increased BER activity post-fertilization*

Following the discovery that a significant contribution of sperm-derived OGG1 to 8OHdG excision post-fertilization is unlikely, further investigation was carried out to characterize the events driving accelerated 8OHdG repair in the zygote. Although increased transcription of OGG1, APE1 or XRCC1 genes post-fertilization would explain the observed elevation in 8OHdG repair, no changes in levels of mRNA or protein relating to any of the BER enzymes could be detected between the MII and zygotic stages (Fig. 5A and B). Further confirmation that the post-fertilization increase in 8OHdG excision was not a consequence of changes in the expression of DNA repair proteins was achieved via exposure to the translation/protein synthesis inhibitor cycloheximide (20 μg/ml) throughout the 5 h incubation. Inhibition of translation throughout this period had no demonstrable effect on levels of 8OHdG excision by the zygote, as detected by the ELISA assay (Fig. 5C).

In light of these data, we next examined the possibility that post-translational modifications, known to strengthen the association between key BER enzymes and accelerate rates of 8OHdG excision (Hu et al., 2005; Almeida and Sobol, 2007), may be controlling this post-fertilization event. This analysis revealed distinct global changes in protein phosphorylation between the MII stage oocyte and the zygote as depicted in Fig. 6. An abundance of phosphorylated cytoplasmic proteins could be identified throughout the ooplasm of both the MII oocyte and zygote by both anti-phospho-serine (Fig. 6A) and anti-phospho-threonine (Fig. 6B) antibodies, with threonine phosphorylation levels being significantly elevated in the zygote ($P < 0.001$) (Fig. 6C). Significantly, these cytoplasmic signals were augmented by a prominent nuclear phosphoprotein signal associated with male and female pronuclei within the zygote (Fig. 6).

This fertilization-triggered association of phosphorylated proteins with the pronuclei was found to extend specifically to enzymes involved in the BER pathway. A Duolink in situ fluorescence proximity ligation assay (PLA) depicted localization of OGG1 phosphorylated at serine and threonine residues to the nuclei of the zygote; while no distinct association with the metaphase plate could be identified in MII oocytes (Fig. 7A and B). Control images have been included that depict low levels of punctate red fluorescence where one antibody has been omitted, and where an antibody not predicted to interact with the antibodies-of-interest (in this case α-tubulin) has been utilized (Fig. 7C). Pixel intensity analysis confirmed that Duolink fluorescence associated with OGG/phospho-serine and OGG1/phospho-threonine was prominently and significantly above that of control oocytes (antibody omitted and OGG1/Tubulin) ($P < 0.001$) (Fig. 7C). In adopting an antibody targeting phospho-XRCC1 (S518, T519, T523) we also identified a uniform cytoplasmic distribution of fluorescence prior to fertilization that became localized to the pronuclei (Fig. 7D) following fertilization. In contrast, no phopho-XRCC1 was found in the vicinity of the metaphase plate in unfertilized MII oocytes (Fig. 7D).

In order to determine the mechanism responsible for relocating these BER enzymes to the pronuclei of freshly fertilized oocytes, the latter were exposed to TBB, an inhibitor known to impair casein kinase 2 (CK2)-directed phosphorylation of XRCC1 (Kubota et al., 2009). Zygotes exposed to TBB experienced a dose-dependent loss of vitality (Fig. 7E); presumably an indication of the vital role that CK2 plays at this stage of development. A dose of 100 μM TBB was finally selected for experiments on CK2 inhibition, as no significant effects on either vitality or fertilization rate were detected at this concentration (Fig. 7E). As hypothesized, zygotes exposed to 100 μM TBB throughout the 5 h incubation period experienced diminished nuclear localization of phospho-XRCC1 (Fig. 7D). Importantly, this decline in phosphorylation of pronuclei-associated XRCC1 was accompanied by a significant reduction in levels 8OHdG excision by the zygote ($P < 0.05$) (Fig. 7F). These results suggested that the elevated levels of 8OHdG excision detected post-fertilization are primarily a result of post-translational modifications to the BER enzymes associated with the nucleus. However, these results do not account for the significantly lower levels of mitochondrial 8OHdG observed in the zygote (when compared to the MII stage oocyte) following H_2O_2 treatment (Fig. 2B, C and E). Thus, we investigated the possibility that an increase in antioxidant protection may accompany fertilization in addition to the pronuclear localization of enzymes involved in the BER pathway.

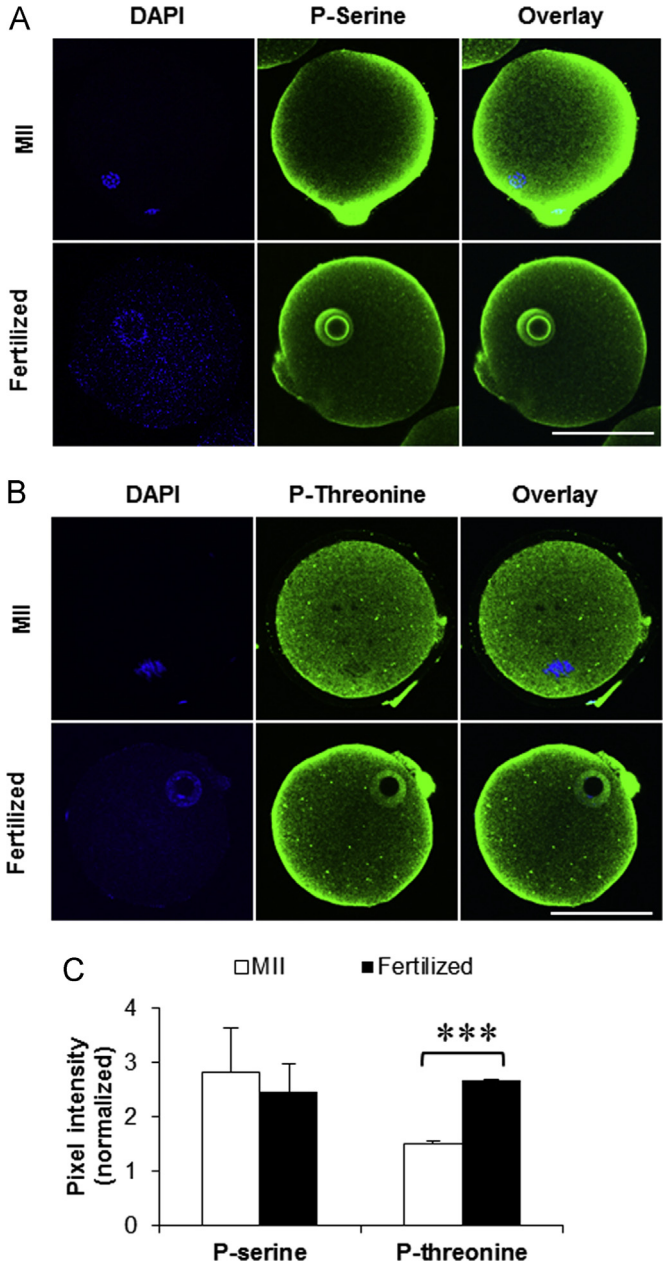

Fig. 6. Fertilization is associated with a shift in the post-translational modification profile of the oocyte. (A) Immunocytochemistry using a phospho-serine antibody revealed a change in expression from the MII stage to the zygote. MII stage oocytes exhibited phospho-serine fluorescence throughout the ooplasm and localized to the plasma membrane, while fluorescence within the zygote was prominently associated with the pronuclei. (B) Similarly, fluorescence associated with the phospho-threonine antibody showed distinct localisation to the pronuclei following fertilization, whilst fluorescence was uniform throughout the cytoplasm in unfertilized MII stage oocytes. (C) Pixel intensity analysis revealed a significant increase in levels of global phospho-threonine expression in zygotes, however no significant difference between levels of phospho-serine expression was detected. Mean ± SEM values are plotted in histograms. Independent replicates were conducted with a minimum of 60 oocytes per replicate. Scale bar = 50 μm. $^{***}P < 0.001$.

3.4. Post-fertilization changes improve antioxidant capacity to protect the zygote from oxidative damage

In order to assess cellular antioxidant capacity, MII stage and fertilized oocytes were exposed to 1 mM H_2O_2 for 1 h before a further 30 min incubation with DFF DA; a live-cell assay that emits fluorescence upon interaction with intracellular oxidants. Interestingly, fertilized oocytes exhibited significantly lower levels of DFF DA fluorescence than MII stage oocytes ($P < 0.01$), suggesting a more rapid breakdown of H_2O_2 (Fig. 8A). An increased capacity for neutralization of harmful oxidants post-fertilization would provide explanation as to the previously described decrease in susceptibility of zygotes to H_2O_2-induced mitochondrial oxidative DNA damage (Fig. 2B, C and E) as well as the reduced likelihood for vitality loss after a 3 h recovery period following H_2O_2 treatment ($P < 0.001$) (Fig. 8B). An analysis of peroxisome abundance using an antibody against peroxisomal membrane protein (PMP70) did not reveal any significant changes within the oocyte following fertilization, suggesting that these catalase-rich organelles were not responsible for the increased H_2O_2 scavenging potential of the fertilized oocyte (Fig. 8C). Contrastingly, antioxidant activity of the enzyme glutathione peroxidase (GPx) was found to be significantly upregulated post-fertilization, with populations of zygotes exhibiting an average rate of activity of 14.7 (±3.9) nmol/min/ml compared to only 7.4 (±2.6) nmol/min/ml in equivalent populations of MII oocytes ($P < 0.01$) (Fig. 8D).

The increase in GPx activity associated with fertilization also prevented the accumulation of cytoplasmic ROS that normally occurs in vitro with increasing periods of time from ovulation (8 h) ($P < 0.01$) (Fig. 8E) and acts as a trigger for oocyte degeneration and apoptosis (Lord et al., 2013, 2015).

4. Discussion

Repair of oxidative DNA lesions such as the highly mutagenic 8OHdG adduct prior to initiating S-phase of the first mitotic division in the zygote is crucial for the preservation of embryonic integrity and the production of healthy offspring. Unfortunately, 8OHdG can be abundant within spermatozoa, particularly within sub-fertile populations, elevating the likelihood that damaged DNA will be contributed to the zygote at fertilization (Aitken et al., 2010). Further to this, the zygote has been demonstrated to possess a restricted capacity for 8OHdG repair, allowing progression through S-phase in the presence of unrepaired oxidative DNA damage (Ronen and Glickman, 2001; Vinson and Hales, 2002; Aitken et al., 2009; Chabory et al., 2009; Takahashi, 2012; Lane et al., 2014). The current manuscript has characterized BER in the mouse pre- S-phase zygote, revealing a low abundance of the first enzyme in the BER pathway, OGG1, thereby explaining the limited capacity for 8OHdG repair at this early developmental stage. Despite the under-representation of OGG1, we have demonstrated BER activity within the oocyte/zygote, the efficiency of which has been found to increase in response to fertilization. Specifically, post-translational modifications of the BER enzymes post-fertilization appear to increase association between these enzymes and the male and female pronuclei, promoting 8OHdG excision from oxidized nuclear DNA. This elevation in 8OHdG repair, although limited, along with a previously undescribed increase in oxidant scavenging activity in fertilized oocytes, are likely to be important not only for minimising levels of mutagenesis in the resulting embryo, but also for redirecting female germ cells away from inevitable senescence and apoptotic death to a developmental pathway associated with cell survival and a commitment to embryogenesis.

The observation that OGG1 is poorly represented at both the transcript and protein level in C57/BL6 × CBA oocytes and zygotes was surprising, as the BER pathway is known to be the primary orchestrator of 8OHdG repair in eukaryotic cells [reviewed by David et al. (2007)]. Additionally, these DNA repair proteins are required within the oocyte throughout oogenesis to control levels of DNA damage, as embryonic gene expression is not initiated until the 2–4 cell stage of embryo development (Flach et al., 1982). Repair of oxidative lesions such as 8OHdG is particularly important

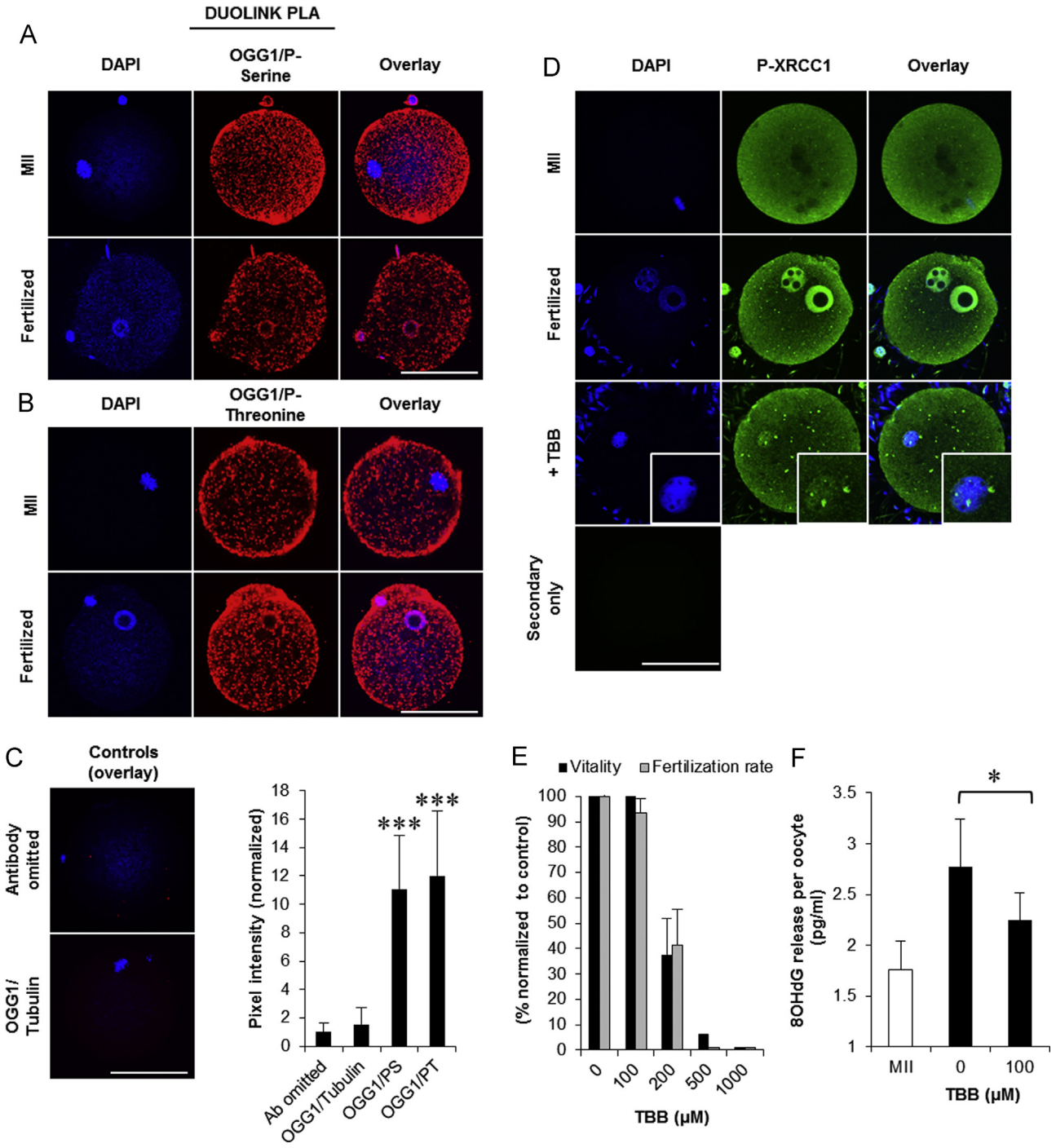

Fig. 7. Post-translational modification of the BER enzymes may co-ordinate increased 8OHdG excision from the nucleus post-fertilization. (A) A proximity ligation assay (PLA) inferred that phosphorylation of OGG1 at serine residues occurs within the genetic material following fertilization, as demonstrated by co-localization between the red punctate fluorescent signal and the DAPI-stained pronuclei of the zygote. Contrastingly, no distinct association could be detected between phosphorylated OGG1 and the metaphase plate in unfertilized oocytes. (B) Similarly, fertilization stimulated phosphorylation of OGG1 at threonine residues within the pronuclei, while no association between phosphorylated OGG1 and the genetic material was detected in MII stage oocytes. (C) Control images (overlay) depict a lack of red punctate fluorescence emanated by the Duolink assay when one antibody was omitted, or when an unrelated antibody was utilized (α-tubulin) in conjunction with our antibody of interest (OGG1). Pixel intensity analysis confirmed significantly elevated levels of fluorescence in OGG1/phospho-serine and OGG1/phospho-threonine replicates above that of the controls. (D) Phosphorylated XRCC1 (S518, T519 and T523) also exhibited cytoplasmic distribution within MII oocytes, while fertilized oocytes showed prominent localisation of P-XRCC1 to the pronuclei. (E) In order to establish the effects of impaired phosphorylation and nuclear localization of XRCC1, a CK2 inhibitor (TBB) was utilized. A dose-dependent study revealed that concentrations of TBB below 200 μM were non-lethal to oocytes/zygotes over a 5 h incubation, and at a concentration of 100 μM did not impair fertilization rate. (F) Exposure to 100 μM TBB throughout fertilization did however result in reduced nuclear localisation of P-XRCC1 in zygotes (D), in conjunction with a significant decline in levels of 8OHdG excision. Mean ± SEM values are plotted in histograms. Independent replicates were conducted with a minimum of 60 oocytes per replicate. Scale bar = 50 μm. $^{*}P < 0.05$, $^{***}P < 0.001$.

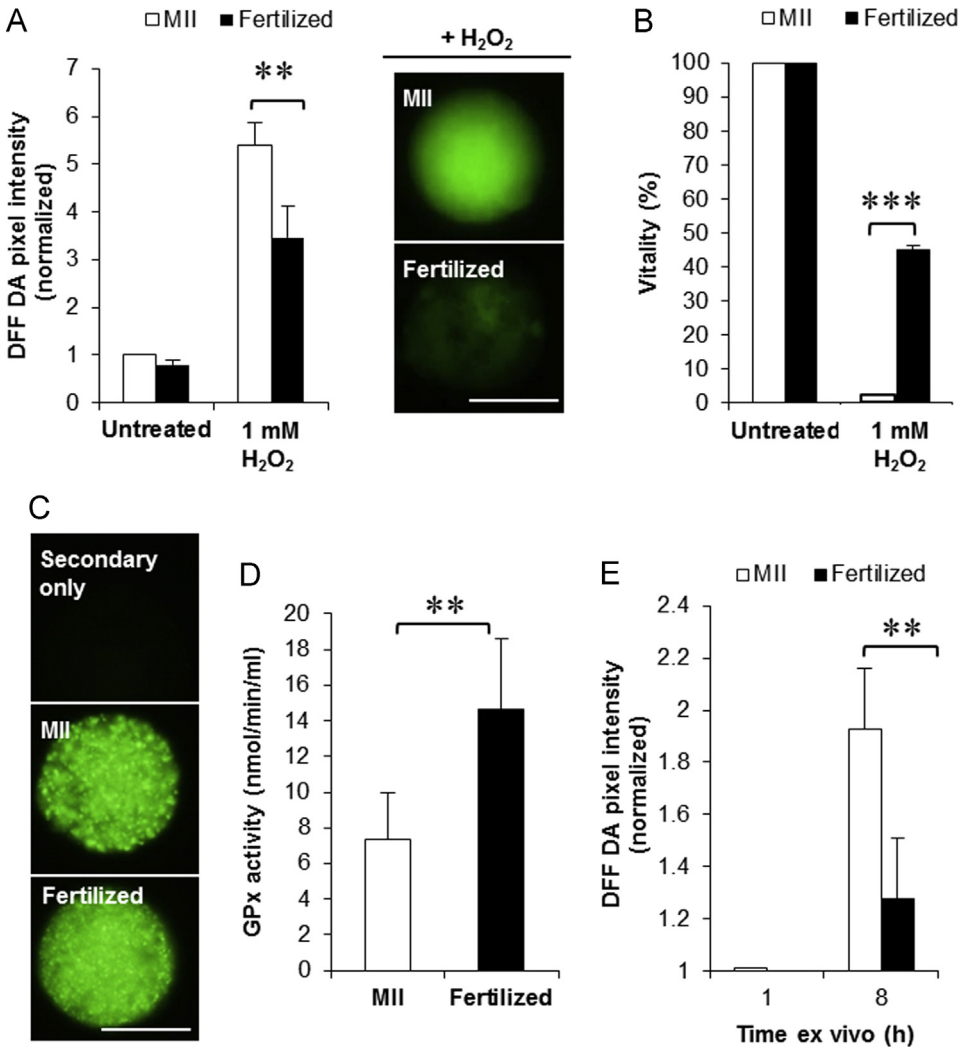

Fig. 8. Fertilization stimulates GPx activity within the oocyte. (A) Populations of MII stage oocytes and zygotes were subjected to a 1 h H_2O_2 challenge, followed by a 30 min recovery in the presence of the fluorescent probe DFF DA. Fertilized oocytes exhibited significantly lower levels of fluorescence when compared to MII stage oocytes, suggesting a more rapid breakdown of H_2O_2. (B) Zygotes were also found to be less susceptible to oxidative stress-induced vitality loss; exhibiting significantly elevated levels of viability above populations of MII stage oocytes following 1 mM H_2O_2 treatment and 3 h recovery time. (C) The improved capacity for H_2O_2 breakdown in zygotes was not associated with increased abundance of catalase-rich peroxisomes, as no change in peroxisome levels were detected following fertilization using an anti- PMP70 antibody. (D) Contrastingly, activity of the antioxidant enzyme GPx was doubled in populations of zygotes when compared to equivalent populations of MII stage oocytes, as determined by a GPx ELISA assay. (E) The characterised up-regulation of GPx activity was also found to prevent the accumulation of ROS within the ooplasm known to be associated with extended periods of in vitro culture (8 h). Mean ± SEM values are plotted in histograms. Independent replicates were conducted with a minimum of 50 oocytes per replicate. $^{**}P < 0.01$, $^{***}P < 0.001$. Scale bar = 50 μm.

at the early stages of zygote development prior to the initiation of mitosis in order to prevent irreversible changes in genetic integrity including transversion mutations (Wood et al., 1992; Bruner et al., 2000; Ohno et al., 2014). As such, the limited availability of this crucial enzyme, OGG1, is likely a contributor to the vulnerability of early mammalian embryos to oxidative DNA damage (Meseguer et al., 2007). Indeed, recent studies have suggested that oxidative DNA damage contributed to the zygote by the fertilizing spermatozoon can directly affect embryo development and quality (Chabory et al., 2009), as well as increase the vulnerability of offspring to pathologies such as metabolic syndrome and obesity (Meseguer et al., 2007; Lane et al., 2014); presumably a consequence of these paternal 8OHdG lesions evading repair by the zygote. It is important to note that although enzymes within alternative DNA repair pathways, such as those of the global genomic NER pathway, are known to be present within the mammalian oocyte (Zheng et al., 2005; Menezo et al., 2007) and are also capable of 8OHdG excision, these enzymes perform long patch repair [up to 13 nucleotides (Melis et al., 2013)] that is normally reserved for 8OHdG lesions that are causative of structural distortions [reviewed by Brierley and Martin (2013)]; thus, these mechanisms are unlikely to significantly contribute to minimising oxidative DNA damage in the zygote. Furthermore, no changes in levels of 8OHdG excision could be identified in this study within the zygote upon inhibition of global genomic and transcription coupled NER using the xeroderma pigmentosum group A (XPA) inhibitor X80 (Neher et al., 2010).

Although there do appear to be limitations to the capacity of the BER enzymes to excise 8OHdG in the oocyte, the current study has characterised a series of mechanisms that are likely to be important for minimising oxidative DNA damage following the union of gametes, thus decreasing the potential for mutagenesis in the embryo. Significantly, within a short window following fertilization (< 5 h), the rate of 8OHdG excision by the BER enzymes was found to be dramatically accelerated. This elevation in BER activity was not related to changes in expression of any of these enzymes, in keeping with the fact that embryonic gene expression is not initiated until the 2–4 cell stage (Flach et al., 1982).

Furthermore, although OGG1 was identified within mouse spermatozoa in this study, as has previously been described in human spermatozoa (Smith et al., 2013b), use of the OGG1-deficient SAMP8 mouse (Smith et al., 2013a) suggested that the sperm-derived enzyme was not significantly contributing to the elevated rate of 8OHdG excision following fertilization. Despite this, the high level of OGG1 expression within spermatozoa is clearly important for maintaining low levels of 8OHdG within the paternal chromatin prior to fertilization. As demonstrated by our expression studies, the oocyte/zygote has an abundance of APE1 and XRCC1 that would – following the union of gametes – allow for swift hydrolysis of abasic sites created by OGG1 in the sperm chromatin, followed by insertion of a new base by DNA polymerase [reviewed by David et al. (2007)].

The mechanism we propose for increasing BER activity following fertilization is via post-translational modification of the BER enzymes. Certainly, the post-translational modification of proteins has been previously shown to be stimulated or accelerated by post-fertilization changes within the murine oocyte allowing for the 'reprogramming' of this cell away from senescence and apoptosis, and towards embryogenesis in the absence of active gene expression and de novo protein translation (Howlett and Bolton, 1985). An abundance of post-translational modifications to the BER enzymes have been characterized previously; some of which increase BER activity, while others exert an inhibitory effect [reviewed by Almeida and Sobol (2007)]. For the purpose of this study, we have focused on phosphorylation of OGG1 and XRCC1. Phosphorylation of OGG1 by cyclin-dependent kinase 4 (Cdk4) at serine/threonine residues is known to accelerate 8OHdG excision twofold (Hu et al., 2005), whilst phosphorylation of XRCC1 at Ser518,Thre519, Thre523 by CK2 is known to instigate nuclear localisation (Parsons et al., 2010), as well as accelerated 8OHdG excision by way of increased interaction with OGG1 and APE1 (Vidal et al., 2001; Marsin et al., 2003; Parsons et al., 2010; Ström et al., 2011). Although no global increases in levels of OGG1 or XRCC1 phosphorylation were identified between the MII and zygotic stages, a distinct nuclear localisation of the signal could be detected following fertilization. This suggests that while BER within the chromatin of the MII stage oocyte is limited, fertilization-associated factors orchestrate phosphorylation of the BER enzymes associated with the nuclei, allowing for accelerated 8OHdG excision and repair prior to the initiation of S-phase and subsequent embryogenesis. By impairing phosphorylation and thus nuclear localisation of XRCC1 using the CK2 inhibitor TBB (Kubota et al., 2009), a significant decline in levels of 8OHdG excision in the zygote was observed (Fig. 7).

In addition to the fertilization-associated elevation in BER activity within the chromatin, this study has also identified an associated increase in antioxidant protection within the zygote. In contrast to unfertilized MII stage oocytes, zygotes demonstrated a superior capacity for H_2O_2 breakdown; suggesting an increase in catalase or GPx bioavailability (Pigeolet et al., 1990). Although no change in abundance of catalase-rich peroxisomes could be detected, an elevation in GPx activity was apparent following fertilization. This elevation in GPx activity was particularly beneficial for protecting the mitochondria from H_2O_2–induced oxidative DNA damage; a biological trait that is acutely important when considering that these mitochondria are to be distributed to every cell within the embryo, and consequently the offspring, and will be primarily responsible for energy production via oxidative phosphorylation (Dumollard et al., 2007), at least until mitochondrial replication following the blastocyst stage of development (St. John et al., 2010). Further to this, the post-fertilization increase in GPx activity would provide protection to the nuclear DNA to prevent the acquisition of any further oxidative lesions prior to the initiation of embryogenesis.

The fertilization-associated mechanisms described in this manuscript are also likely to be a component of the 'molecular switch' that rescues the MII stage oocyte from otherwise inevitable entry into a post-ovulatory ageing/apoptotic cascade, redirecting this cell into a developmental pathway. In the absence of fertilization, the oocyte experiences an accumulation of ROS with increasing amounts of time post-ovulation (Lord et al., 2013, 2015). This oxidative stress and associated damage is known to be a direct trigger for degeneration and the initiation of age-associated apoptosis in the mammalian oocyte (Kujoth et al., 2006; Lord et al., 2013, 2015). Importantly, the current study has demonstrated that fertilized oocytes are resistant to this time-dependent accumulation of ROS, presumably as a consequence of upregulated GPx activity. By preventing the accumulation of ROS and associated oxidative damage, these fertilization-associated events effectively redirect the oocyte away from the default apoptotic pathway that inevitably occurs in the absence of fertilization, and allow for unimpeded embryo development.

In conclusion, the results depicted in this study suggest that a series of strategies are in place to minimise levels oxidative DNA damage in the mammalian zygote and thus the mutational load ultimately carried by the embryo. Firstly, expression of OGG1 in the spermatozoon will serve to minimise levels of 8OHdG contributed to the OGG1-deficient oocyte, instead presenting abasic sites that can readily be rectified by the abundance of APE1 and XRCC1 in the ooplasm. Additionally, in response to fertilization, the maternal BER machinery accelerates 8OHdG excision in the pronuclei as a consequence of post-translational modifications, while an increase in antioxidant activity protects the entire embryo from the acquisition of any further oxidative damage. Despite this, we propose that when OGG1 within the sperm cell is overwhelmed, for example, in the spermatozoa of sub-fertile men exhibiting high levels of 8OHdG (De Iuliis et al., 2009), then the oocyte has a limited capacity to excise these potentially mutagenic adducts following fertilization. When the burden of oxidative damage is too high in the OGG1-deficient oocyte, consequences can include arrest or disruption of the normal developmental process (Ronen and Glickman, 2001; Vinson and Hales, 2002; Aitken et al., 2009; Chabory et al., 2009; Takahashi, 2012; Lane et al., 2014). In a clinical context, this study further highlights the concerns associated with using ART techniques such as ICSI on unscreened subfertile patients that potentially harbor high levels of oxidative DNA damage within their spermatozoa.

Acknowledgments

A special thanks to Aimee Katen for her assistance with PCR analysis. Also, we are very grateful to the NHMRC (Grant no. 494802) for their financial support.

Appendix A. Supplementary material

Supplementary material associated with this article can be found in the online version at http://dx.doi.org/10.1016/j.ydbio.2015.07.024.

References

Aitken, R.J., De Iuliis, G.N., 2010. On the possible origins of DNA damage in human spermatozoa. Mol. Hum. Reprod. 16, 3–13.

Aitken, R.J., De Iuliis, G.N., Finnie, J.M., Hedges, A., McLachlan, R.I., 2010. Analysis of the relationships between oxidative stress, DNA damage and sperm vitality in a patient population: development of diagnostic criteria. Hum. Reprod. 25, 2415–2426.

Aitken, R.J., De Iuliis, G.N., McLachlan, R.I., 2009. Biological and clinical significance of DNA damage in the male germ line. Int. J. Androl. 32, 46–56.
Aitken, R.J., Paterson, M., Fisher, H.M., Buckingham, D.W., Van Duin, M., 1995. Redox regulation of tyrosine phosphorylation in human spermatozoa and its role in the control of human sperm function. J. Cell Sci. 108 (Pt 5), 2017–2025.
Almeida, K.H., Sobol, R.W., 2007. A unified view of base excision repair: lesion-dependant protein complexes regulated by post-translational modification. DNA Repair 6, 695–711.
Braude, P.R., Bolton, V.N., Moore, S., 1988. Human gene expression first occurs between the four and eight cell stages of preimplantation development. Nature 332, 459–461.
Brierley, D.J., Martin, S.A., 2013. Oxidative stress and the DNA mismatch repair pathway. Antioxid. Redox Signal. 18, 2420–2428.
Bruner, S.D., Norman, D.P.G., Verdine, G.L., 2000. Structural basis for recognition and repair of the endogenous mutagen 8-oxoguanine in DNA. Nature 403, 859–866.
Chabory, E., Damon, C., Lenoir, A., Kauselmann, G., Kern, H., Zevnik, B., Garrel, C., Saez, F., Cadet, R., Henry-Berger, J., Schoor, M., Gottwald, U., Habenicht, U., Drevet, J.R., Vernet, P., 2009. Epididymis seleno-independent glutathione peroxidase 5 maintains sperm DNA integrity in mice. J. Clin. Invest. 119, 2074–2085.
Choi, J.Y., Kim, H.S., Kang, H.K., Lee, D.W., Choi, E.M., Chung, M.H., 1999. Thermolabile 8-hydroxyguanine DNA glycosylase with low activity in senescence-accelerated mice due to a single-base mutation. Free Radic. Biol. Med. 27, 848–854.
David, S.S., O'Shea, V.L., Kundu, S., 2007. Base-excision repair of oxidative DNA damage. Nature 447, 941–950.
De Iuliis, G.N., Thomson, L.K., Mitchell, L.A., Finnie, J.M., Koppers, A.J., Hedges, A., Nixon, B., Aitken, R.J., 2009. DNA damage in human spermatozoa is highly correlated with the efficiency of chromatin remodeling and the formation of 8-hydroxy-2'-deoxyguanosine a marker of oxidative stress. Biol. Reprod. 81, 517–524.
Dumollard, R., Ward, Z., Carroll, J., Duchen, M.R., 2007. Regulation of redox metabolism in the mouse oocyte and early embryo. Development 134, 455–465.
Flach, G., Johnson, M.H., Braude, P.R., Taylor, R.A., Bolton, V.N., 1982. The transition from maternal to embryonic control in the 2-cell mouse embryo. EMBO J. 1, 681–686.
Howlett, S.K., Bolton, V.N., 1985. Sequence and regulation of morphological and molecular events during the first cell cycle of mouse embryogenesis. J. Embryol. Exp. Morphol. 87, 175–206.
Hu, J., Imam, S.Z., Hashiguchi, K., De Souza-Pinto, N.C., Bohr, V.A., 2005. Phosphorylation of human oxoguanine DNA glycosylase (alpha-OGG1) modulates its function. Nucleic Acids Res. 33, 3271–3282.
Kubota, Y., Takanami, T., Higashitani, A., Horiuchi, S., 2009. Localization of X-ray cross complementing gene 1 protein in the nuclear matrix is controlled by casein kinase II-dependent phosphorylation in response to oxidative damage. DNA Repair 8, 953–960.
Kujoth, G.C., Leeuwenburgh, C., Prolla, T.A., 2006. Mitochondrial DNA mutations and apoptosis in mammalian aging. Cancer Res. 66, 7386–7389.
Lane, M., McPherson, N.O., Fullston, T., Spillane, M., Sandeman, L., Kang, W.X., Zander-Fox, D.L., 2014. Oxidative stress in mouse sperm impairs embryo development, fetal growth and alters adiposity and glucose regulation in female offspring. PLoS One 9, e100832.
Lord, T., Martin, J.H., Aitken, R.J., 2015. Accumulation of electrophilic aldehydes during post-ovulatory ageing of mouse oocytes causes reduced fertility, oxidative stress and apoptosis. Biol Reprod. 92, 1–13.
Lord, T., Nixon, B., Jones, K.T., Aitken, R.J., 2013. Melatonin prevents post-ovulatory oocyte aging in the mouse and extends the window for optimal fertilization in vitro. Biol Reprod. 88, 1–9.
Madhusudan, S., Smart, F., Shrimpton, P., Parsons, J.L., Gardiner, L., Houlbrook, S., Talbot, D.C., Hammonds, T., Freemont, P.A., Sternberg, M.J.E., Dianov, G.L., Hickson, I.D., 2005. Isolation of a small molecule inhibitor of DNA base excision repair. Nucleic Acids Res. 33, 4711–4724.
Marsin, S., Vidal, A.E., Sossou, M., Murcia, J.M., Le Page, F., Boiteux, S., de Murcia, G., Radicella, J.P., 2003. Role of XRCC1 in the coordination and stimulation of oxidative DNA damage repair initiated by the DNA glycosylase hOGG1. J. Biol. Chem. 278, 44068–44074.
Melis, J.P.M., Steeg, H., Luijten, M., 2013. Oxidative DNA damage and nucleotide excision repair. Antioxid. Redox Signal. 18, 2409–2419.
Menezo, Y., Russo, G., Tosti, E., Mouatassim, S.E., Benkhalifa, M., 2007. Expression profile of genes coding for DNA repair in human oocytes using pangenomic microarrays, with a special focus on ROS linked decays. J. Assist. Reprod. Genet. 24, 513–520.
Meseguer, M., Martinez-Conejero, J.A., O'Connor, J.E., Pellicer, A., Remohi, J., Garrido, N., 2007. The significance of sperm DNA oxidation in embryo development and reproductive outcome in an oocyte donation program: a new model to study a male infertility prognostic factor. Fertil. Steril. 89, 1191–1199.
Neher, T.M., Shuck, S.C., Liu, J., Zhang, J., Turchi, J.J., 2010. Identification of novel small molecule inhibitors of the XPA protein using in silico based screening. ACS Chem. Biol. 5, 953–965.
O'Flaherty, C., De Lamirande, E., Gagnon, C., 2006. Positive role of reactive oxygen species in mammalian sperm capacitation: triggering and modulation of phosphorylation events. Free Radic. Biol. Med. 41, 528–540.
Ohno, M., Sakumi, K., Fukumura, R., Furuichi, M., Iwasaki, Y., Hokama, M., Ikemura, T., Tsuzuki, T., Gondo, Y., Nakabeppu, Y., 2014. 8-oxoguanine causes spontaneous de novo germline mutations in mice. Sci. Rep. 4, 4689.
Parsons, J.L., Dianova, I.I., Finch, D., Tait, P.S., Ström, C.E., Helleday, T., Dianov, G.L., 2010. XRCC1 phosphorylation by CK2 is required for its stability and efficient DNA repair. DNA Repair 9, 835–841.
Pigeolet, E., Corbisier, P., Houbion, A., Lambert, D., Michiels, C., Raes, M., Zachary, M., Remacle, J., 1990. Glutathione peroxidase, superoxide dismutase, and catalase inactivation by peroxides and oxygen derived free radicals. Mech. Ageing Dev. 51, 283–297.
Rivlin, J., Mendel, J., Rubinstein, S., Etkovitz, N., Breitbart, H., 2004. Role of hydrogen peroxide in sperm capacitation and acrosome reaction. Biol. Reprod. 70, 518–522.
Ronen, A., Glickman, B.W., 2001. Human DNA repair genes. Environ. Mol. Mutagen. 37, 241–283.
Schneider-Poetsch, T., Ju, J., Eyler, D.E., Dang, Y., Bhat, S., Merrick, W.C., Green, R., Shen, B., Liu, J.O., 2010. Inhibition of eukaryotic translation elongation by cycloheximide and lactimidomycin. Nat. Chem. Biol. 6, 209–217.
Shimura, T., Inoue, M., Taga, M., Shiraishi, K., Uematsu, N., Takei, N., Yuan, Z.M., Shinohara, T., Niwa, O., 2002. p53-dependent S-phase damage checkpoint and pronuclear cross talk in mouse zygotes with X-irradiated sperm. Mol. Cell Biol. 22, 2220–2228.
Smith, T.B., De Iuliis, G.N., Lord, T., Aitken, R.J., 2013a. The senescence-accelerated mouse prone 8 (SAMP8) as a model for oxidative stress and impaired DNA repair in the male germ line. Reproduction 146, 253–262.
Smith, T.B., Dun, M.D., Smith, N.D., Curry, B.J., Connaughton, H.S., Aitken, R.J., 2013b. The presence of a truncated base excision repair pathway in human spermatozoa, mediated by OGG1. J. Cell Sc. 126 (Pt 6), 1488–1497.
Sobinoff, A.P., Beckett, E.L., Jarnicki, A.G., Sutherland, J.M., McClusky, A., Hansbro, P. M., McLaughlin, E.A., 2013. Scrambled and fried: cigarette smoke exposure causes antral follicle destruction and oocyte dysfunction through oxidative stress. Toxicol. Appl. Pharmacol. 271, 156–167.
St. John, J.C., Facucho-Oliveira, J., Jiang, Y., Kelly, R., Salah, R., 2010. Mitochondrial DNA transmission, replication and inheritance: a journey from the gamete through the embryo and into offspring and embryonic stem cells. Hum. Reprod. Update 16, 488–509.
Ström, C.E., Mortusewicz, O., Finch, D., Parsons, J.L., Lagerqvist, A., Johansson, F., Schultz, N., Erixon, K., Dianov, G.L., Helleday, T., 2011. CK2 phosphorylation of XRCC1 facilitates dissociation from DNA and single-strand break formation during base excision repair. DNA Repair 10, 961–969.
Takahashi, M., 2012. Oxidative stress and redox regulation on in vitro development of mammalian embryos. J. Reprod. Dev. 58, 1–9.
Vidal, A.E., Boiteux, S., Hickson, I.D., Radicella, J.P., 2001. XRCC1 coordinates the initial and late stages of DNA abasic site repair through protein-protein interactions. EMBO J. 20, 6530–6539.
Vinson, R.K., Hales, B.F., 2002. DNA repair during organogenesis. Mutat. Res. 509, 79–91.
Wood, M.L., Esteve, A., Morningstar, M.L., Kuziemko, G.M., Essigmann, J.M., 1992. Genetic effects of oxidative DNA damage: comparative mutagenesis of 7,8-dihydro-8-oxoguanine and 7,8-dihydro-8-oxoadenine in Escherichia coli. Nucleic Acids Res. 20, 6023–6032.
Wu, B.J., Yin, L.J., Yin, H.P., Ying, X.S., Yang, W.W., Zeng, Y.M., Zhu, J., Kang, X.D., Liu, G.J., Yu, L.P., Gu, M.E., Wu, P.L., 2013. A mutation in the Kit gene leads to novel gonadal phenotypes in both heterozygous and homozygous mice. Hereditas 147, 62–69.
Zheng, P., Schramm, R.D., Latham, K.E., 2005. Developmental regulation and in vitro culture effects on expression of DNA repair and cell cycle checkpoint control genes in rhesus monkey oocytes and embryos. Biol. Reprod. 72, 1359–1369.